Huygens-Fresnel principle for surface plasmons

Tatiana Teperik, Alexandre Archambault, François Marquier, Jean-Jacques Greffet

Huygens-Fresnel principle for surface plasmons

T. V. Teperik[1,2,*], A. Archambault[1], F. Marquier[1], and J. J. Greffet[1]

[1] *Laboratoire Charles Fabry de l'Institut d'Optique, CNRS and Université Paris-Sud, Campus Polytechnique, RD 128, 91127 Palaiseau cedex, France*

[2] *On leave from: Institute of Radio Engineering and Electronics (Saratov Division), Russian Academy of Sciences, Zelyonaya 38, 410019 Saratov, Russia*

[*] *tatiana.teperik@institutoptique.fr*

Abstract: We present an explicit form of the surface plasmon propagator. Its form has the structure of a vectorial Huygens-Fresnel principle. The propagator appears to be a powerful tool to deal with diffraction, interference and focusing of surface plasmons. In contrast with the scalar approximation used so far, the vectorial propagator accounts for near-field and polarization effects. We illustrate the potential of the propagator by studying diffraction of surface plasmons by a slit and focusing of surface plasmons by a Fresnel lens.

OCIS codes: (240.6680) Surface plasmons; (070.7345) Fourier optics and signal processing: Wave propagation; (260.3910) Metal optics

References and links

1. E. Ozbay, "Plasmonics: Merging Photonics and Electronics at Nanoscale Dimensions," Science **311**, 189–193 (2006).
2. W. L. Barnes, A. Dereux, and T. W. Ebbesen, "Surface plasmon subwavelength optics," Nature **424**, 824–830 (2003).
3. H. Raether, *Surface Plasmons*, Springer Tracts Mod. Phys., Vol.111 (Springer, Berlin, Heidelberg, 1988).
4. I. I. Smolyaninov, C. C. Davis, and A. V. Zayats, "Image formation in surface plasmon polariton mirrors: applications in high-resolution optical microscopy," New J. Phys. **7**, 175(1)–175(7) (2005).
5. I. I. Smolyaninov, J. Elliott, A. V. Zayats, and C. C. Davis, "Far-Field Optical Microscopy with a Nanometer-Scale Resolution Based on the In-Plane Image Magnification by Surface Plasmon Polaritons," Phys. Rev. Lett. **94**, 057,401(1)–057,401(4) (2005).
6. A. B. Evlyukhin, S. I. Bozhevolnyi, A. L. Stepanov, R. Kiyan, C. Reinhardt, S. Passinger, and B. N. Chichkov, "Focusing and directing of surface plasmon polaritons by curved chains of nanoparticles," Opt. Express **15**, 667–680 (2007).
7. A. Drezet, D. Koller, A. Hohenau, A. Leitner, F. R. Aussenegg, and J. R. Krenn, "Surface plasmon polariton microscope with parabolic reflectors," Opt. Lett. **32**, 2414–2416 (2007).
8. Z. Liu, J. M. Steele, W. Srituravanich, Y. Pikus, C. Sun, and X. Zhang, "Focusing Surface Plasmons with a Plasmonic Lens," Nano Lett. **5**, 1726–1729 (2005).
9. L. Yin, V. K. Vlasko-Vlasov, J. Pearson, J. M. Hiller, J. Hua, U. Welp, D. E. Brown, and C. W. Kimball, "Subwavelength Focusing and Guiding of Surface Plasmons," Nano Lett. **5**, 1399–1402 (2005).
10. L. Verslegers, P. B. Catrysse, Z. Yu, J. S. White, E. S. Barnard, M. L. Brongersma, and S. Fan, "Planar Lenses Based on Nanoscale Slit Arrays in a Metallic Film," Nano Lett. **9**, 235–238 (2009).
11. L. Feng, K. A. Tetz, B. Slutsky, V. Lomakin, and Y. Fainman, "Fourier plasmonics: Diffractive focusing of in-plane surface plasmon polariton waves," Appl. Phys. Lett. **91**, 081,101(1)–081,101(3) (2007).
12. A. G. Curto and F. J. García de Abajo, "Near-Field Optical Phase Antennas for Long-Range Plasmon Coupling," Nano Lett. **8**, 2479–2484 (2008).
13. A. J. Huber, Deutsch, L. Novotny, and R. Hillenbrand, "Focusing of surface phonon polaritons," Appl. Phys. Lett. **92**, 203,104(1)–203,104(3) (2008).
14. R. Zia and M. L. Brongersma, "Surface plasmon polariton analogue to Youngs double-slit experiment," Nature Nanotechnol. **2**, 426–429 (2007).

#114297 - $15.00 USD Received 14 Jul 2009; revised 14 Aug 2009; accepted 30 Aug 2009; published 15 Sep 2009

15. J.-Y. Laluet, E. Devaux, C. Genet, T. W. Ebbesen, J.-C. Weeber, and A. Dereux, "Optimization of surface plasmons launching from subwavelength hole arrays: modelling and experiments," Opt. Express **15**, 3488–3495 (2007).
16. J. J. Greffet and R. Carminati, "Image formation in near-field optics," Progress in Surface Science **56**, 133–237, (1997).
17. J. A. Porto, R. Carminati, and J.-J. Greffet, "Theory of electromagnetic field imaging and spectroscopy in scanning near-field optical microscopy," J. Appl. Phys. **88**, 4845–4850 (2000).
18. A. V. Zayats, I. I. Smolyaninov, A. A. Maradudin, "Nano-optics of surface plasmon polaritons," Phys. Reports **408**, 131-314 (2005)
19. J. N. Walford, J. A. Porto, R. Carminati, and J.-J. Greffet, "Theory of near-field magneto-optical imaging," J. Opt. Soc. Am. A **19**, 572–583 (2002).
20. A. Archambault, T. V. Teperik, F. Marquier, and J. J. Greffet, "Surface plasmon Fourier optics," Phys. Rev. B **79**, 195,414(1)–195,414(8).
21. W. Zhu, A. Agrawal, and Ajay Nahata, "Direct measurement of the Gouy phase shift for surface plasmon-polaritons," Opt. Express **15**, 9995–10001 (2007).
22. I. I. Smolyaninov, D. L. Mazzoni, J. Mait, and C. C. Davis, "Experimental study of surface-plasmon scattering by individual surface defects," Phys. Rev. B **56**, 1601–1611 (1997).
23. P. B. Johnson and R. W. Christy, "Optical constants of the noble metals," Phys. Rev. B **6**, 4370–4379 (1972).
24. A. Drezet, A. Hohenau, and J. R. Krenn, "Comment on Far-Field Optical Microscopy with a Nanometer-Scale Resolution Based on the In-Plane Image Magnification by Surface Plasmon Polaritons," Phys. Rev. Lett. **98**, 209,703(1) (2007).
25. Y. Li and E. Wolf, "Focal shifts in diffracted converging spherical waves," Opt. Commun. **39**, 211–215 (1981).
26. M. P. Givens, "Focal shifts in diffracted converging spherical waves," Opt. Commun. **41**, 145–148 (1982).

1. Introduction

Recent advances in nanofabrication and the desire to miniaturize photonic circuits have renewed the interest in plasmonics [1, 2]. The unique dispersive properties of surface plasmons lead to particularities in propagation, interference and diffraction as compared with light. Despite a strong analogy between surface plasmons and light, a general framework to deal with surface plasmon propagation is still missing. We will show that the basic principles of Fourier optics developed for light propagation in a vacuum can be extended to surface plasmons. This will provide an adequate framework for dealing with surface-plasmons optical systems.

The dispersion relation for a surface plasmon propagating along a planar metal surface $z = 0$ bounded by a dielectric can be written in the form [3]:

$$k_{SP}^2 = k_x^2 + k_y^2 = \frac{\omega^2}{c^2}\frac{\varepsilon_1\varepsilon_2(\omega)}{\varepsilon_1+\varepsilon_2(\omega)}, \tag{1}$$

where ε_1 is the dielectric constant of the environment, $\varepsilon_2(\omega)$ is the frequency-dependent dielectric function of the metal, and c is the speed of light. In the long-wavelength regime the dispersion of surface plasmons slightly deviates from the light line $k = \omega\sqrt{\varepsilon_1}/c$, while in the short wavelength regime the surface plasmon dispersion is strongly modified and tends to an asymptotic non-retarded solution. In the case of the Drude model, it is given by $\omega_p/\sqrt{\varepsilon+1}$, where ω_p is the bulk plasma frequency [3]. Thus, one can expect significant deviations between light and surface-plasmon diffraction in the short wavelength regime.

As for photons, focusing of surface plasmons is the result of constructive and destructive interference. It is expected that surface plasmons can produce highly localized spots as their wavelength can be much shorter than the wavelength of light in surrounding media. On the other hand, these surface plasmons are expected to decay very rapidly in space, preventing them to produce an image at a large distance. Focusing of surface plasmons with different types of lenses has been studied by many groups [4, 5, 6, 7, 8, 9, 10, 11, 12]. Furthermore, the focusing of surface phonon polaritons - surface waves formed by the strong coupling of light and optical phonons in polar crystals - has been reported in [13]. The lens configuration can strongly influence the intensity of focal spot as well as the quality of the resolution. Thus, it is

#114297 - $15.00 USD Received 14 Jul 2009; revised 14 Aug 2009; accepted 30 Aug 2009; published 15 Sep 2009

of interest to analyse the properties of Fresnel lens [11] that is expected to be one of the most effective surface plasmon focusing device.

Until now, the problem of diffraction and focusing of surface plasmons has been modeled theoretically either using numerical models [11] or scalar approximations [4, 14, 15]. Although the scalar approximation reveals the physics behind the phenomena observed in experiments and provides a qualitative agreement with the measured images [4, 11, 14, 15], it fails to account for polarization effects. The polarization is important when anaysing images [16, 17, 18]. Indeed, an experimental observation of surface plasmons based on far-field scattering is mostly related to the longitudinal (in-plane) component whereas an aperture-less near-field microscope image yields an image related to the transverse component of the electric field [17, 19].

In this paper we derive the exact form of the vectorial propagator of the surface-plasmon field. This provides a rigorous foundation for surface-plasmon Fourier optics. Using this propagator, one can analyse the potential and limitations of surface-plasmon imaging. To illustrate the use of the propagator, we discuss diffraction of a surface-plasmon field by a slit and we compare the results with the scalar approximation. This comparison shows a further limitation of the scalar approximation. It proves to be reliable only for distances larger than a wavelength whereas the exact propagator is valid at any distance. We also discuss imaging using a Fresnel lens. Finally, we examine the resolution limit, the focal shift, and the effect of losses.

2. Huygens-Fresnel principle for surface plasmons

We consider the propagation of a monochromatic surface plasmon field along a planar surface $z = 0$ in the direction of postive x. The time dependence $\exp(-i\omega t)$ is omitted for brevity. Our starting point is a general representation of the surface plasmon field on a flat interface derived in [20]:

$$\mathbf{E}^{SP}(x,y) = \int \frac{dk_y}{2\pi}\, \mathbf{E}^{SP}(k_y) e^{i\sqrt{k_{SP}^2 - k_y^2}x + ik_y y}. \tag{2}$$

We have omitted the z-dependence of the field given by $\exp(i\sqrt{\varepsilon_1\omega^2/c^2 - k_{SP}^2}\, z)$ in the upper medium and by $\exp(-i\sqrt{\varepsilon_2\omega^2/c^2 - k_{SP}^2}\, z)$ in the metal. Indeed, the decay along the z-axis depends on the frequency but not on k_y. This expansion is analogous to the angular plane wave representation of fields in a vacuum. It is valid for $x > 0$ in a source free region. We note that the three components of the electric field in the dielectric can be expressed in terms of the z-component: $(E_x(k_y) = \sqrt{k_{SP}^2 - k_y^2}\,\frac{k_z}{k_{SP}^2} E_z^{SP}(k_y)$, $E_y(k_y) = k_y \frac{k_z}{k_{SP}^2} E_z^{SP}(k_y)$, $E_z^{SP}(k_y))$, where $k_z = \sqrt{\varepsilon_1\omega^2/c^2 - k_{SP}^2}$ is the z-component of the wavevector in dielectric environment. We observe that the integral in Eq.(2) is the Fourier transform of the product of two functions of k_y. For example, for the z-component, they are $E_z^{SP}(k_y)$ and $\exp(i\sqrt{k_{SP}^2 - k_y^2}x)$. It can thus be written as a convolution product in direct space. Making use of the integral representation of the Hankel function we obtain the helpful relation

$$\int \mathrm{d}k_y\, e^{i\sqrt{k_{SP}^2 - k_y^2}x + ik_y y} = -i\pi \frac{\partial}{\partial x} H_0^{(1)}(k_{SP}\rho)$$

where $\rho = \sqrt{x^2 + y^2}$. Equation (2) can be cast in the form

$$\mathbf{E}^{SP}(x,y) = \int dy'\, E_z^{SP}(x = 0, y')\mathbf{K}(x, y - y'), \tag{3}$$

#114297 - $15.00 USD Received 14 Jul 2009; revised 14 Aug 2009; accepted 30 Aug 2009; published 15 Sep 2009

where

$$\mathbf{K}(x,y-y') = \begin{bmatrix} K_x \\ K_y \\ K_z \end{bmatrix} = -\frac{1}{2} \begin{bmatrix} \frac{k_z}{k_{SP}^2} \frac{\partial^2}{\partial x^2} H_0^{(1)}(k_{SP}\rho) \\ \frac{k_z}{k_{SP}^2} \frac{\partial^2}{\partial x \partial y} H_0^{(1)}(k_{SP}\rho) \\ i \frac{\partial}{\partial x} H_0^{(1)}(k_{SP}\rho) \end{bmatrix}, \tag{4}$$

is the vectorial surface plasmon propagator and $\rho = \sqrt{x^2 + (y-y')^2}$. Equation (3) can be viewed as a vectorial Huygens-Fresnel principle for surface plasmons. Indeed, the surface plasmon field at (x,y) appears to result from the interferences of surface plasmons emitted by secondary sources located at $(x = 0, y')$ with an amplitude $E_z^{SP}(x = 0, y')$. It should be noted that Eq. (3) yields the complex amplitude of surface plasmon field from which the phase of the surface plasmon field can be easily extracted. Thus the Huygens-Fresnel principle derived for surface plasmons can be considered as a simple and elegant tool for study such effect as Gouy phase shift [21] avoiding time consuming numerical simulations.

In order to see more clearly the link with Huygens-Fresnel principle, we use the asymptotic form of the Hankel function, valid for distances larger than the wavelength. We obtain:

$$\begin{aligned} &E_z^{SP}(x,y) = \\ &\quad = -\tfrac{i}{\sqrt{\lambda_{SP}}} \int dy' \, \cos\theta \, E_z^{SP}(x=0,y') \frac{e^{ik_{SP}\rho}}{\sqrt{\rho}} e^{i\pi/4}, \end{aligned} \tag{5}$$

where $\lambda_{SP} = 2\pi/k_{SP}$ is the surface plasmon wavelength and $\theta = \arccos(x/\rho)$. Here, the propagator is a damped cylindrical wave $e^{ik_{SP}\rho}/\sqrt{\rho}$ instead of the spherical wave e^{ikr}/r in the case of light propagation in a 3D vacuum. We recover in this asymptotic regime a surface plasmon form that has been conjectured previously [4, 22]. However, let us emphasize two differences between the scalar approximation and the propagator given by Eq. (3). Firstly, Eq. (3) is valid for any distance and includes near-field terms. Secondly, Eq. (3) and Eq. (4) shows that the x and y components of the electric field can be derived from the z-component. More specifically, the parallel components of the field are given by $E_x = \frac{k_z}{k_{SP}^2} \frac{\partial E_z}{\partial x}$, $E_y = \frac{k_z}{k_{SP}^2} \frac{\partial E_z}{\partial y}$. In the next section we compare Eq. (5) and Eq.(3).

3. Diffraction of surface plasmons by a slit

To illustrate the potential of the exact form of the propagator, we first discuss the diffraction of a surface plasmon by a slit of width $w = 6\lambda_{sp}$. We consider that a homogeneous surface plasmon propagates along the glass/gold interface in the x-direction. We describe the dielectric function of gold $\varepsilon_2(\omega)$ using experimental data [23]. To calculate the diffraction pattern of the surface plasmon diffracted by a slit, we use Eq. (3) and the so-called Kirchhoff or physical optics approximation. This approximation assumes that the field in the aperture ($|y| < w/2$) is set equal to the incident field and vanishes outside the aperture ($|y| > w/2$).

Figure 1 shows the intensity distribution of surface plasmon field normalized by the intensity of the z-component of the incident surface plasmon field. The diffraction pattern closely resembles the intensity patterns of light diffracted by a slit. Following the intensity versus x along the line $y = 0$ in Figs. 1(a) and (c), one observes that the intensity oscillates exhibiting the wave nature of the surface plasmon. The diffraction patterns for the x and z components are very similar and their amplitudes are comparable in this example. When changing the frequency, the relative amplitude changes. Moreover, it is seen in Fig. 1(b) that the intensity of the y component of the surface plasmon field is 100 times less than that of the z-component. This component is only due to diffraction. It can be increased by reducing the slit width. Finally, a

#114297 - $15.00 USD Received 14 Jul 2009; revised 14 Aug 2009; accepted 30 Aug 2009; published 15 Sep 2009

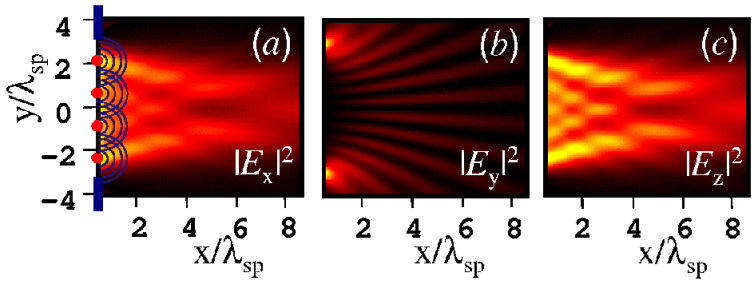

Fig. 1. Diffraction pattern of a slit with width $w = 6\lambda_{sp}$ illuminated from the left by a homogeneous surface plasmon at normal incidence. $\lambda_{sp} = 400$ nm. The intensity is normalized by the intensity of the z-component of the incident surface plasmon field at x=0. Black is zero intensity. Yellow indicates the maximum intensity and corresponds to 0.25 in (a) 0.01 in (b), and 1.2 in (c).

comparison between Figs. 1(a), (b) and (c) shows that the diffracted surface plasmon field has different intensity distributions for each component so that it can hardly be treated as a scalar field [4, 14].

We have compared the asymptotic solution Eq. (5) proposed earlier [4, 22] with the general Huygens-Fresnel principle Eq. (3) derived in this paper. Figure 2 shows the intensity of the z-component of the surface-plasmon field normalized to the intensity of the z-component of the incident surface plasmon field calculated through the center of a slit ($y = 0$). We have found that the asymptotic solution Eq. (5) (black curve in Fig. 2) and the general solution Eq. (3) (red curve in Fig. 2) coincide in the radiation zone ($\rho > \lambda_{SP}$). For a distance $\rho \approx \lambda_{SP}/10$, the intensity obtained using Eq. (3) is half as much again the intensity obtained when using the asymptotic form of the Hankel function. This is of practical importance. Indeed, due to the ohmic damping of surface plasmons, many applications are in the intermediate regime between the near field and radiation zones.

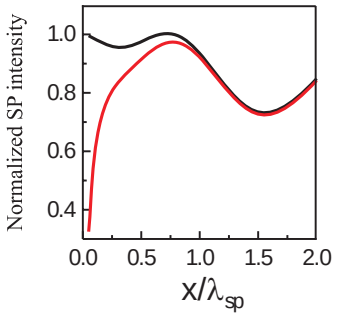

Fig. 2. The intensity of z-component of surface plasmon field normalized to the intensity of the z-component of the incident surface plasmon field calculated at $y = 0$ using the general Huygens-Fresnel principle Eq. (3) (black curve) and the asymptotic solution Eq. (5) (red curve). The others parameters are the same as on Fig. 1.

4. Focusing of surface plasmons by a Fresnel lens

As a second example of application of the propagator, we consider the design of a Fresnel lens for surface plasmons. The lens consists in a series of apertures centered at $y_j =$

#114297 - $15.00 USD Received 14 Jul 2009; revised 14 Aug 2009; accepted 30 Aug 2009; published 15 Sep 2009

$\sqrt{(|j|\lambda_{SP}+f)^2-f^2}$, $j=-n,...,n$, where f is the focal distance as shown in Fig. 3(a). The width of each slit is chosen in such a way that the optical path difference of surface plasmons coming from opposite edges of the same slit is equal to $\lambda_{SP}/6$. This is a tradeoff between a large width to ensure a large transmission and a small width to ensure a good coherence. In Figs. 3(b-e) we show the surface plasmon intensity distribution, $I=|E_x^{SP}|^2+|E_y^{SP}|^2+|E_z^{SP}|^2$, normalized to the intensity of the z-component of the incident surface plasmon field for several surface plasmon wavelengths. When illuminating by a homogeneous surface plasmon at normal incidence, the fields diffracted by the slits interfere constructively at the focal point [see Figs. 3(b-d)]. The number of slits $N=2n+1$ is chosen to provide the maximum possible intensity at the focal point. Due to ohmic losses for surface plasmons, a further increase in N does not change the intensity distribution because the contribution from remote slits is negligible due to the finite surface plasmon propagation length. As one can see in Fig. 4(a), increasing the number of slits does not increase the intensity beyond a cut-off number that depends on the wavelength.

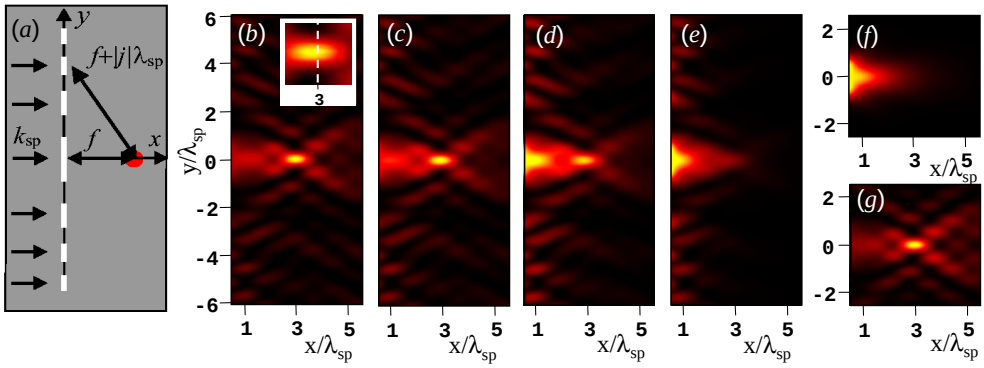

Fig. 3. (a) Schematically the metal surface and the diffraction of surface plasmons by a Fresnel lens. (b-e) The intensity of the diffracted surface plasmon field $I=|E_x^{SP}|^2+|E_y^{SP}|^2+|E_z^{SP}|^2$ normalized to the intensity of the z-component of the incident surface plasmon field. The homogeneous surface plasmon propagating along the glass/gold interface with the wavelength (b) $\lambda_{sp}=400$ nm, (c) 375 nm (d) 350 nm (e) 325 nm impinges the lens from the left. The Fresnel lens has the focal distance $f=3\lambda_{sp}$ and composed from non-periodical array of slits. The number of slits is $N=2n+1$, $n=13$. The inset in figure (b) shows a detail of focal spot. (f) the diffraction of surface plasmon $\lambda_{sp}=325$ nm by a single slit of the width $w=2\lambda_{sp}$. (g) the same as (e) with no losses. The color scale is different for each pattern and indicates as black the zero intensity and yellow the maximum intensity (b) 3.21, (c) 2.22, (d) 1.31, (e) 1.07, (f) 1.11 (g) 5.53.

We now address the issue of resolution using surface plasmons. It has been argued in previous studies that the resolution is limited when using surface plasmons on lossy metals [5, 24]. In our simulations, we observe that the size of the image focal spot in Figs.3 (b) and (c) is smaller than the vacuum wavelength. However, it is limited to roughly half of the surface plasmon wavelength. This result agrees with the analysis of ref. [20] where it is stated that there is a maximum wavevector k_{SP} given by the turning point of the surface plasmon dispersion with backbending. This limit implies that there is also a limit to the maximum intensity that can be achieved by focusing a surface plasmon. In Fig. 4(a) we show that the field intensity at the focus of the Fresnel lens saturates when the number of slits increases. This is due to the the attenuation of surface plasmons emitted by slits several decay lengths away. Figure 4(b) shows that for a given size of a lens, there is an optimal focal distance, at which the maximum

#114297 - $15.00 USD Received 14 Jul 2009; revised 14 Aug 2009; accepted 30 Aug 2009; published 15 Sep 2009

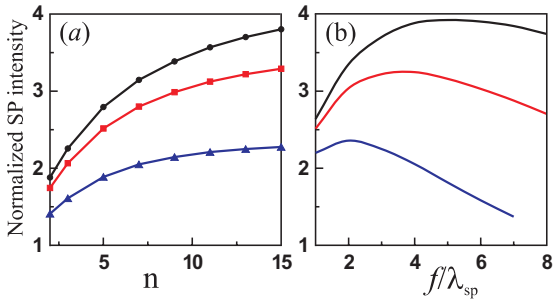

Fig. 4. (a) Normalized intensity of surface plasmon field diffracted by a Fresnel lens made of an array of $N = 2n+1$ slits with a focal distance $f = 3\lambda_{sp}$ versus n. (b) Normalized intensity of the surface plasmon field diffracted by a Fresnel lens made of a nonperiodical array of $N = 2n+1$ slits, $n = 13$, as a function of the focal distance f. The calculation has been performed for the different surface plasmon wavelengths: $\lambda_{sp} = 435$ nm (black circles (a), black curve (b)), 400 nm (red squares (a), red curve (b)) 375 nm (blue triangles (a) and blue curve (b)). The lines in figure (a) are for eyes guidance.

intensity is achieved. Thus, from Fig. 4 one can deduce that there is a set of parameters at which the Fresnel lens operates most effectively.

A potential interest of surface plasmon is to produce high resolution in the proximity of the asymptote of the dispersion relation where small surface plasmon wavelengths can be achieved. However, as one can see in Fig. 3(e), the short wavelength surface plasmons do not exhibit any focusing. This is due to the increased dissipation of the surface plasmons. In the short surface plasmon wavelength regime, the Fresnel lens cannot operate as a focusing device and is nothing but a nonperiodic array of slits through which the surface plasmon diffracts. The secondary surface plasmons launched from the slits do not exhibit any interference because the decay length is smaller than the wavelength. It is interesting to compare the diffraction of a surface plasmon by a single slit in Fig. 3(f) and by a Fresnel lens in Fig. 3(e). It is seen that the intensity close to the central aperture is not modified by the other slits. Obviously, one could restore the focus by omitting the losses in the metal as seen in Fig. 3(g). In summary, the resolution is limited by half of a surface plasmon wavelength but the smallest wavelengths decay too rapidly to allow focusing. There is a tradeoff between these effects.

The tradeoff between interference and damping is responsible for a focal shift effect that we discuss in this paragraph. As can be seen in the inset of Fig. 3(b), the point of maximum intensity of the surface plasmon field does not coincide with the geometrical focus f. It is shifted by $\approx \lambda_{sp}/10$ towards the lens aperture. A similar effect has been discussed for light focusing by a number of authors [25, 26]. It can be explained in the framework of Huygens-Fresnel principle in terms of a competition between two opposite trends. On the one hand, the intensity should be maximum when the contributions from all the secondary sources on the aperture interfere constructively. This happens exactly at the geometrical focus by Fresnel lens construction. On the other hand, each surface plasmon decays as $e^{-Imk_{sp}\rho}/\sqrt{\rho}$ [see Eq. (5)] so that if the observation point moves towards the lens aperture, the amplitude increases. The tradeoff between these two effects produces a maximum of intensity which is shifted from the geometrical focus towards the lens aperture. This focal shift is much more pronounced for surface plasmons than for free space light since the amplitude of the spherical wave e^{ikr}/r, which is the propagator for the light, has a weaker $1/r$ decay. We have verified (not shown) that the shift is larger for the surface plasmons with large damping at shorter wavelengths.

#114297 - $15.00 USD Received 14 Jul 2009; revised 14 Aug 2009; accepted 30 Aug 2009; published 15 Sep 2009

5. Conclusion

We have obtained an exact form of the propagator for surface plasmons. In contrast with the scalar approximation used previously, it has the form of a generalized Huygens-Fresnel principle for surface plasmons that includes near-field and polarization effects. In this framework, we have studied surface plasmon propagation, diffraction by a slit, and focusing by a Fresnel lens. The exact propagator provides a rigorous framework to develop Fourier optics for surface plasmons.

Acknowledgments

This work was supported by the French National Research Agency (ANR) through Carnot Leti funding and by the French Ministry of Defense through a grant from the *Direction générale de l'armement* (DGA).

#114297 - $15.00 USD Received 14 Jul 2009; revised 14 Aug 2009; accepted 30 Aug 2009; published 15 Sep 2009